

Implication of the proton electric FF space-like behavior puzzle in various physical phenomena

A.Z.Dubníčková¹ and S.Dubníčka²

¹*Dept. of Theoretical Physics, Comenius Univ., Bratislava, Slovak Republic*

²*Institute of Physics, Slovak Academy of Sciences, Bratislava, Slovak Republic*

(Dated: October 24, 2018)

By means of the 10-resonance unitary and analytic model of nucleon electromagnetic structure it is demonstrated that the JLab proton polarization data on the ratio $\mu_p G_{Ep}(Q^2)/G_{Mp}(Q^2)$ are consistent with all form factor properties, however, they strongly require an existence of the zero in $G_{Ep}(Q^2)$ around $Q^2 = 13\text{GeV}^2$. As a result there are two contradicting behaviors of $G_{Ep}(Q^2)$ in space-like region. Consequences of this phenomenon on the charge distribution within the proton, on the saturation of the new proton-neutron q^2 -dependent sum rule, on the behavior of strange nucleon form factors and the deuteron elastic structure functions through the impulse approximation are investigated.

I. INTRODUCTION

In the framework of the naive quark model the proton is compound of three-quarks and in electromagnetic (EM) interactions they manifest the proton (equally well the neutron) EM structure.

As a result, one doesn't know explicit form of the nucleon matrix element of the EM current

$$J_\mu^{EM} = 2/3\bar{u}\gamma_\mu u - 1/3\bar{d}\gamma_\mu d - 1/3\bar{s}\gamma_\mu s. \quad (1)$$

Then EM form factors (FF), two independent scalar functions of one variable $t = -Q^2$ (the squared four-momentum transferred by the exchanged virtual photon) are introduced to represent the proton EM structure.

There is some freedom in the choice of them.

The most natural is an introduction of Dirac $F_{1p}(t)$ and Pauli $F_{2p}(t)$ FF's

$$\langle p | J_\mu^{EM} | p \rangle = \bar{u}(p') \left\{ \gamma_\mu F_{1p}(t) + i \frac{\sigma_{\mu\nu} q_\nu}{2m_p^2} F_{2p}(t) \right\} u(p). \quad (2)$$

The most suitable in the extraction of experimental information on the proton EM structure are Sachs electric $G_{Ep}(t)$ and magnetic $G_{Mp}(t)$ FFs of the proton

$$\begin{aligned} G_{Ep}(t) &= F_{1p}(t) + \frac{t}{4m_p^2} F_{2p}(t) \\ G_{Mp}(t) &= F_{1p}(t) + F_{2p}(t) \end{aligned} \quad (3)$$

giving in the Breit frame the charge and magnetization distributions within the proton, respectively.

However, for a construction of models of proton EM structure the iso-scalar and iso-vector Dirac and Pauli FF's are the most appropriate, which are defined by the relations

$$\langle N | J_\mu^{I=0} | N \rangle = \bar{u}(p') \{ \gamma_\mu F_1^{I=0}(t) + i \frac{\sigma_{\mu\nu} q_\nu}{2m_p^2} F_2^{I=0}(t) \} u(p) \quad (4)$$

$$J_\mu^{I=0} = \frac{1}{6} (\bar{u} \gamma_\mu u + \bar{d} \gamma_\mu d) - \frac{1}{3} \bar{s} \gamma_\mu s \quad (5)$$

and

$$\langle N | J_\mu^{I=1} | N \rangle = \bar{u}(p') \{ \gamma_\mu F_1^{I=1}(t) + i \frac{\sigma_{\mu\nu} q_\nu}{2m_p^2} F_2^{I=1}(t) \} u(p) \quad (6)$$

$$J_\mu^{I=1} = \frac{1}{2} (\bar{u} \gamma_\mu u - \bar{d} \gamma_\mu d). \quad (7)$$

Iso-scalar and iso-vector Dirac and Pauli FFs, as one can see from the expressions

$$\begin{aligned} G_{Ep}(t) &= [F_1^{I=0}(t) + F_1^{I=1}(t)] + \frac{t}{4m_p^2} [F_2^{I=0}(t) + F_2^{I=1}(t)]; \\ G_{Mp}(t) &= [F_1^{I=0}(t) + F_1^{I=1}(t)] + [F_2^{I=0}(t) + F_2^{I=1}(t)]; \\ G_{En}(t) &= [F_1^{I=0}(t) - F_1^{I=1}(t)] + \frac{t}{4m_n^2} [F_2^{I=0}(t) - F_2^{I=1}(t)]; \\ G_{Mn}(t) &= [F_1^{I=0}(t) - F_1^{I=1}(t)] + [F_2^{I=0}(t) - F_2^{I=1}(t)], \end{aligned} \quad (8)$$

are related separately neither to proton, nor to neutron, but to the nucleons generally. So, one has always to analyze both, proton and neutron, existing experimental data sets by constructed models simultaneously.

II. EXPERIMENTAL INFORMATION ON NUCLEON EM FORM FACTORS

Between the discovery of proton EM structure in the middle of the 1950's till 2000, abundant proton EM FF data (from DESY, SLAC and Bonn) in the space-like region ($t < 0$) appeared (see Fig.1).

They have been obtained from the measured cross section of the elastic scattering of unpolarized electrons on unpolarized protons in the laboratory reference frame

$$\begin{aligned} \frac{d\sigma^{lab}(e^- p \rightarrow e^- p)}{d\Omega} &= \frac{\alpha^2 \cos^2(\theta/2)}{4E^2 \sin^4(\theta/2)} \frac{1}{1 + (\frac{2E}{m_p}) \sin^2(\theta/2)} \cdot \\ &\quad [A(t) + B(t) \tan^2(\theta/2)], \end{aligned} \quad (9)$$

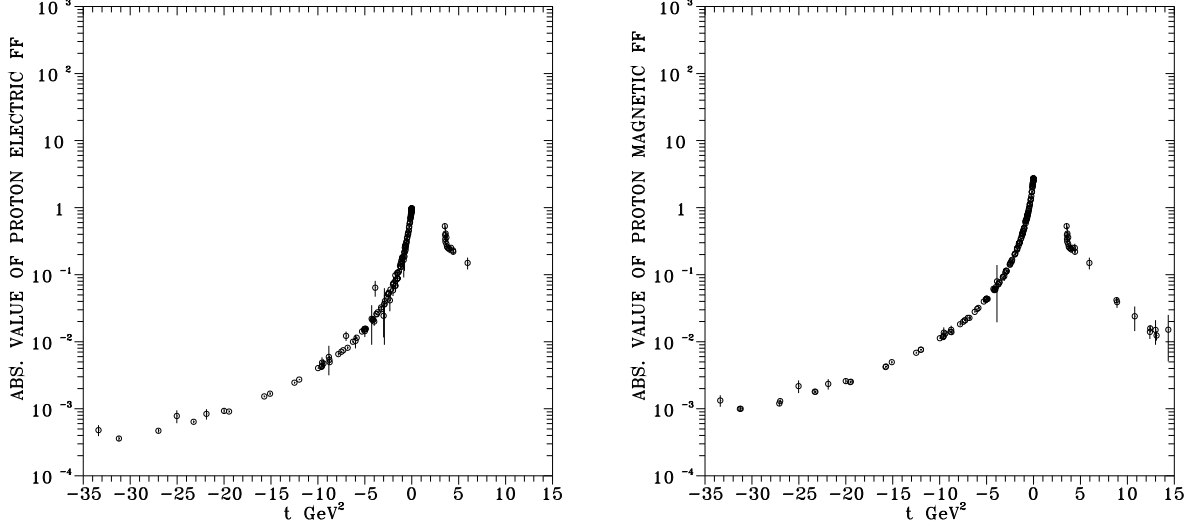


FIG. 1: Experimental data on proton electric and magnetic form factors.

where $\alpha = 1/137$, E -the incident electron energy

$$A(t) = \frac{G_{Ep}^2(t) - \frac{t}{4m_p^2}G_{Mp}^2(t)}{1 - \frac{t}{4m_p^2}}, \quad (10)$$

$$B(t) = -2\frac{t}{4m_p^2}G_{Mp}^2(t) \quad (11)$$

by Rosenbluth technique.

One can see from the previous formulas, that the proton magnetic FF is multiplied by $-t/(4m_p^2)$ factor, i.e. as $-t$ increases, the measured cross-section (9) becomes dominant by $G_{Mp}^2(t)$ part contribution, making the extraction of $G_{Ep}^2(t)$ more and more difficult. So, one can have a confidence only in the proton magnetic FF data obtained by the Rosenbluth technique.

By a slightly more complicated method the neutron electric and magnetic FF's data have been obtained as presented in Fig.2

References on the experimental data on proton and neutron electromagnetic FF's, obtained by Rosenbluth technique, can be found in [1].

More recently at Jefferson Lab [2], [3] measuring simultaneously transverse

$$P_t = \frac{h}{I_0}(-2)\sqrt{\tau(1+\tau)}G_{Mp}G_{Ep}\tan(\theta/2) \quad (12)$$

and longitudinal

$$P_l = \frac{h(E+E')}{I_0m_p}\sqrt{\tau(1+\tau)}G_{Mp}^2\tan^2(\theta/2) \quad (13)$$

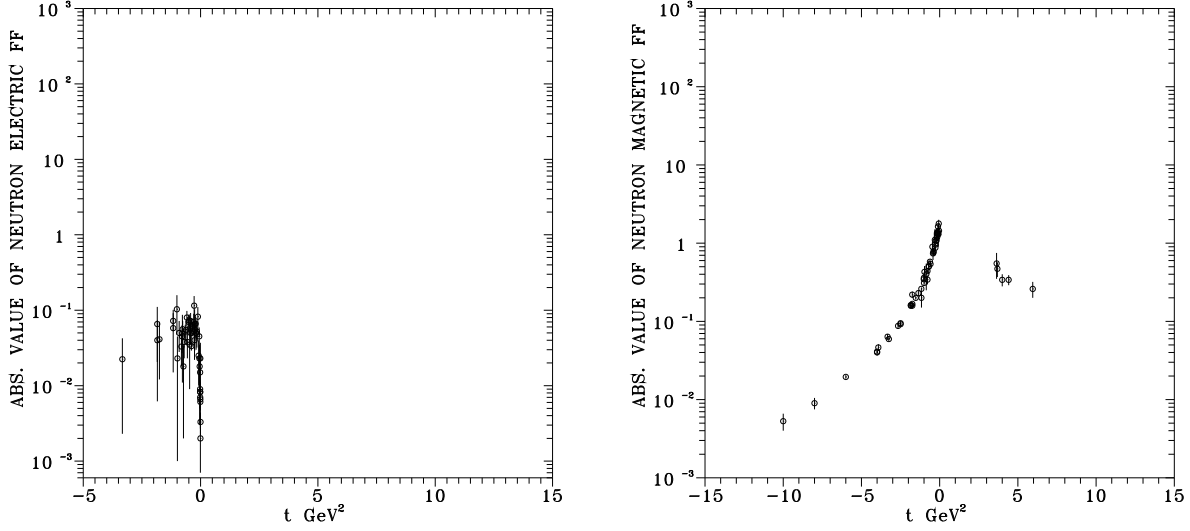


FIG. 2: Experimental data on neutron electric and magnetic form factors.

components of the recoil proton's polarization in the electron scattering plane of the polarization transfer process $\vec{e}^- p \rightarrow e^- \vec{p}'$, where h is the electron beam helicity, I_0 is the unpolarized cross-section excluding σ_{Mott} and $\tau = Q^2/4m_p^2$, the data on the ratio

$$G_{Ep}/G_{Mp} = -\frac{P_t}{P_l} \frac{(E + E')}{2m_p} \tan(\theta/2) \quad (14)$$

were obtained.

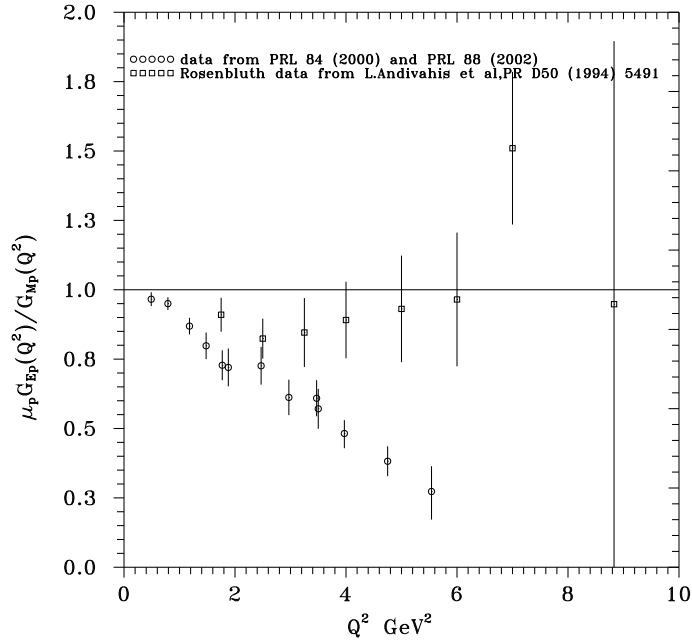


FIG. 3: JLab polarization data on the ratio $\mu_p G_{Ep}(t)/G_{Mp}(t)$

They are in strong disagreement with data obtained by Rosenbluth technique.

Taking into account the dominance of $G_M^p(t)$ in the unpolarized cross-section, we already conjecture the behavior of $G_E^p(t)$ is responsible for the appeared discrepancy.

This conclusion is supported also in the analysis by our Unitary & Analytic (U&A) model of nucleon electromagnetic structure [1].

III. RESULTS OF ANALYZES BY 10-RESONANCE U&A MODEL OF NUCLEON EM STRUCTURE

We have achieved simultaneous description of all existing proton and neutron FF data in space-like and time-like regions by 10-resonance U&A model of nucleon EM structure [1] formulated in the language of iso-scalar $F_{1,2}^s(t)$ and iso-vector $F_{1,2}^v(t)$ Dirac and Pauli FFs, saturating them by $\omega, \phi, \omega', \omega'', \phi'$ and $\rho, \rho', \rho'', \rho''', \rho''''$, respectively.

The model comprises all known nucleon FF properties

- experimental fact of a creation of unstable vector meson resonances in electron-positron annihilation processes into hadrons
- analytic properties of FFs
- reality conditions
- unitarity conditions
- normalizations
- asymptotic behaviors as predicted by the quark model of hadrons.

First, the analysis of all proton and neutron data obtained by Rosenbluth technique, together with all proton and neutron data in time-like region were carried out.

Then, all $G_{Ep}(t)$ space-like data obtained by Rosenbluth technique were substituted for the new JLab proton polarization data on the ratio $\mu_p G_{Ep}(Q^2)/G_{Mp}(Q^2)$ in the interval $0.49 GeV^2 \leq Q^2 \leq 5.54 GeV^2$ and analyzed together with all electric proton time-like data and all space-like and time-like magnetic proton, as well as electric and magnetic neutron, data [4],[5].

The results are presented in Figs.4 and 5.

From these Figures two consequences follow:

- The fact, that almost nothing is changed in a description of $G_{En}(t)$, $G_{Mn}(t)$ and $G_{Mp}(t)$ in both, the space-like and time-like regions, and also $|G_{Ep}(t)|$ in the time-like region, supports

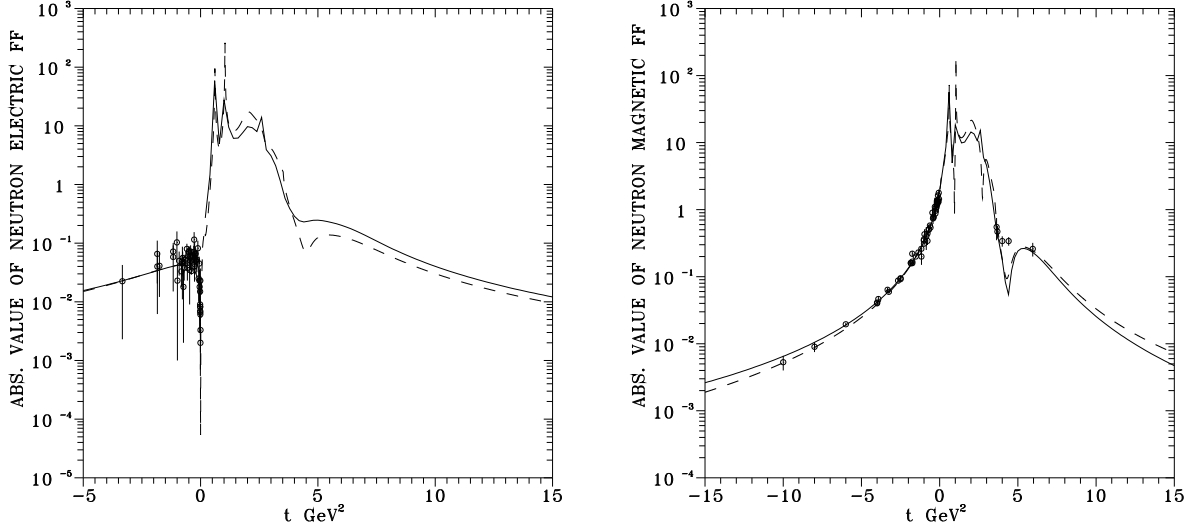


FIG. 4: Theoretical behavior of neutron electric and magnetic form factors.

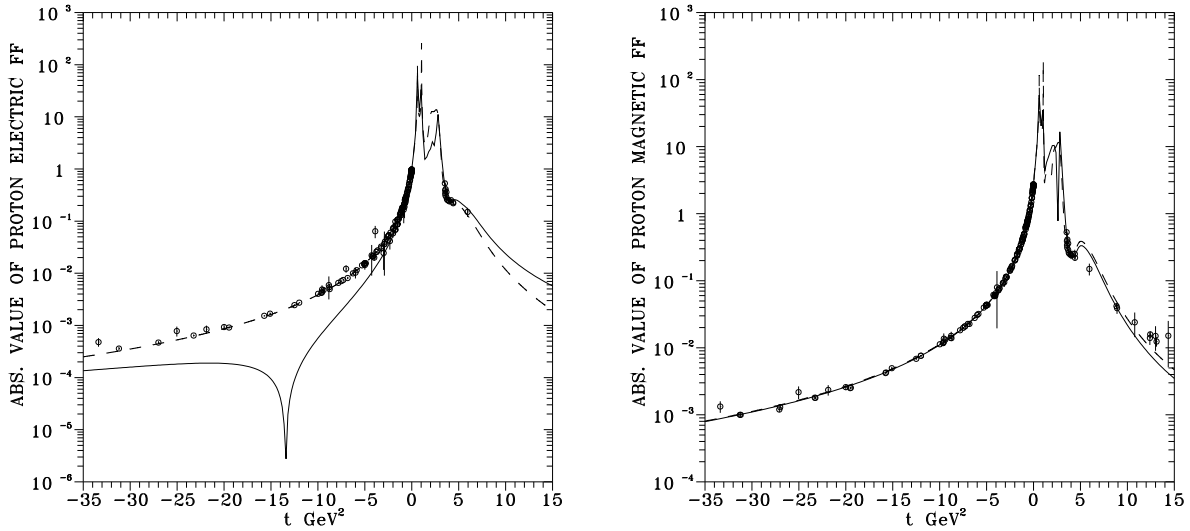


FIG. 5: Theoretical behavior of proton electric and magnetic form factors.

our hypothesis, that the discrepancy between the calculated old and measured new ratios $G_{Ep}(t)/G_{Mp}(t)$ is really created by different behaviors of $G_{Ep}(t)$.

- The new behavior of $G_{Ep}(t)$ (the full line in Fig.5) extracted from the JLab polarization data on $G_{Ep}(t)/G_{Mp}(t)$ is consistent with all known FF properties, including also the asymptotic behavior, but strongly requires an existence of FF zero around $t = -13\text{GeV}^2$.

As a result of our analysis there are two sets of nucleon FF data differing by $G_{Ep}(t)$ behavior in $t < 0$ region.

We would like to note, that the expressions for $\frac{d\sigma^{lab}(e^-p \rightarrow e^-p)}{d\Omega}$ and P_t, P_l are calculated in the

one photon exchange approximation to be justified theoretically.

IV. ATTEMPTS TO SOLVE THE PROBLEM

Despite the fact, that the one photon exchange approximation is justified theoretically, there were attempts to solve the problem by inclusion of additional radiative correction terms, related to two-photon exchange approximations [6],[7],[8],[9],[10].

The analysis revealed:

- the two-photon exchange has a much smaller effect on the polarization transfer than on the Rosenbluth extractions
- the size of the two-photon exchange correction is less than half the size necessary to explain discrepancy

then the problem is still open, though JLab proton polarization data seem to be more reliable.

V. CONSEQUENCES ON CHARGE DISTRIBUTION WITHIN PROTON

The proton charge distribution (assuming to be spherically symmetric) is an inverse Fourier transform of the proton electric FF

$$\rho_p(r) = \frac{1}{(2\pi)^3} \int e^{-iQr} G_{Ep}(Q^2) d^3Q \quad (15)$$

from where

$$\rho_p(r) = \frac{4\pi}{(2\pi)^3} \int_0^\infty G_{Ep}(Q^2) \frac{\sin(Qr)}{Qr} Q^2 dQ. \quad (16)$$

Substituting for the $G_{Ep}(Q^2)$ under the integral:

- either the Rosenbluth behavior
- or the JLab polarization behavior of $G_{Ep}(Q^2)$ with the zero

one gets different charge distributions within the proton given in Fig.6 by dashed and full lines, respectively.

That all leads also to different mean square proton charge radii. The old proton charge radius takes the value $\langle r_p^2 \rangle = 0.68 \text{fm}^2$. If JLab proton polarization data are correct then the new charge radius $\langle r_p^2 \rangle = 0.72 \text{fm}^2$ is larger.

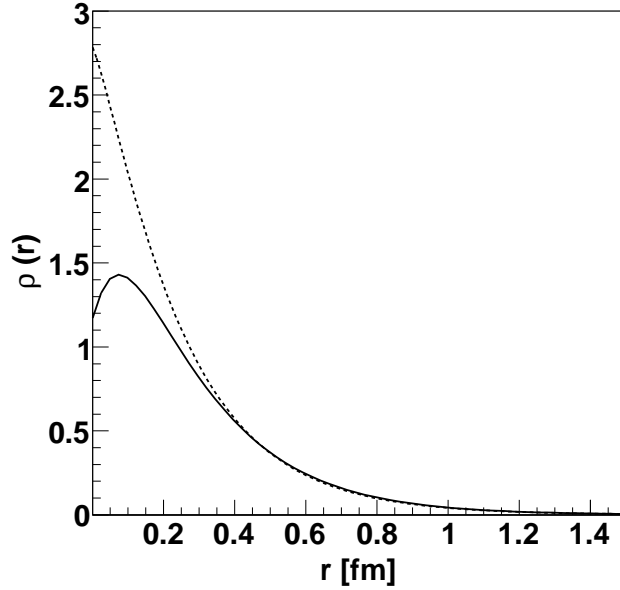


FIG. 6: Charge distribution behavior within the proton

VI. POSSIBLE INSIGHT BY DIS

So, the Jlab proton polarization data strongly require an existence of the zero, i.e. the diffraction minimum in the space-like region of $|G_{Ep}(t)|$ around $t = -Q^2 = 13GeV^2$.

Is really the new predicted $t < 0$ behavior of $G_{Ep}(t)$ in $t < 0$ correct ?

It seems to us that this question could be verified also by DIS, using the new sum rule [11]

$$F_{1p}^2(-\mathbf{q}^2) + \frac{\mathbf{q}^2}{4m_p^2} F_{2p}^2(-\mathbf{q}^2) - F_{1n}^2(-\mathbf{q}^2) - \frac{\mathbf{q}^2}{4m_n^2} F_{2n}^2(-\mathbf{q}^2) = 1 - 2 \frac{(\mathbf{q}^2)^2}{\pi\alpha^2} \left(\frac{d\sigma^{e^-p \rightarrow e^-X}}{d\mathbf{q}^2} - \frac{d\sigma^{e^-n \rightarrow e^-X}}{d\mathbf{q}^2} \right) \quad (17)$$

giving into a relation:

- nucleon electromagnetic form factors
- with difference of deep inelastic electron-proton and electron-neutron differential cross-sections.

By measurements of the right hand side of (17) the true $t < 0$ behavior of the electric proton FF could be chosen

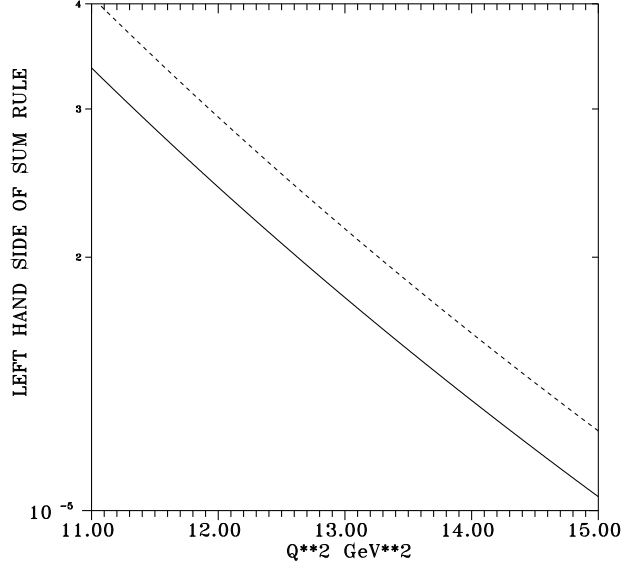


FIG. 7: Q^2 square dependence sum rules results

VII. SENSITIVITY OF STRANGE NUCLEON FFs FROM TWO DIFFERENT BEHAVIORS OF $G_E^p(Q^2)$

The momentum dependence of the nucleon matrix element of the strange-quark vector current $J_\mu^s = \bar{s}\gamma_\mu s$ is contained in the Dirac $F_1^s(t)$ and Pauli $F_2^s(t)$ strange nucleon FFs

$$\langle p' | \bar{s}\gamma_\mu s | p \rangle = \bar{u}(p') \left[\gamma_\mu F_1^s(t) + i \frac{\sigma_{\mu\nu} q^\nu}{2m_N} F_2^s(t) \right] u(p) \quad (18)$$

or in the strange electric and strange magnetic nucleon FFs

$$G_E^s(t) = F_1^s(t) + \frac{t}{4m_N^2} F_2^s(t), \quad G_M^s(t) = F_1^s(t) + F_2^s(t), \quad (19)$$

which, as a consequence of the isospin zero value of the strange quark, contribute only to the behavior of the isoscalar nucleon FFs and never to isovector ones.

Further we will predict the nucleon strange FFs behavior by 8-resonance U&A model and look for distinctive features.

So, the nucleon Dirac and Pauli strange FFs $F_1^s(t)$, $F_2^s(t)$ can be found just from the behavior of $F_1^{I=0}(t)$, $F_2^{I=0}(t)$. The main idea of a prediction of strange nucleon FFs behavior is based:

- on the $\omega - \phi$ mixing to be valid also for coupling constants between EM (quark) current and vector meson

$$\begin{aligned} \frac{1}{f_\omega} &= \frac{1}{f_{\omega_0}} \cos \epsilon - \frac{1}{f_{\phi_0}} \sin \epsilon \\ \frac{1}{f_\phi} &= \frac{1}{f_{\omega_0}} \sin \epsilon + \frac{1}{f_{\phi_0}} \cos \epsilon \end{aligned} \quad (20)$$

- on the assumption that the quark current of some flavor couples with universal strength κ exclusively to the vector-meson wave function component of the same flavor

$$\langle 0 | \bar{q}_r \gamma_\mu q_r | (\bar{q}tq_t)_V \rangle = \kappa m_V^2 \delta_{rt} \varepsilon_\mu \quad (21)$$

which result in the relations

$$\begin{aligned} (f_{\omega NN}^{(i)}/f_\omega^s) &= -\sqrt{6} \frac{\sin \varepsilon}{\sin(\varepsilon + \theta_0)} (f_{\omega NN}^{(i)}/f_\omega^e) \\ (f_{\phi NN}^{(i)}/f_\phi^s) &= -\sqrt{6} \frac{\cos \varepsilon}{\cos(\varepsilon + \theta_0)} (f_{\phi NN}^{(i)}/f_\phi^e) \\ (i &= 1, 2) \end{aligned} \quad (22)$$

where f_ω^s, f_ϕ^s are strange-current $\leftrightarrow V = \omega, \phi$ coupling constants and $\varepsilon = 3.7^\circ$ is a deviation from the ideally mixing angle $\theta_0 = 35.3^\circ$.

So, if one knows from the fit of nucleon FF data free parameters $(f_{\omega NN}^{(i)}/f_\omega^e), (f_{\phi NN}^{(i)}/f_\phi^e)$ ($i=1,2$) of the suitable model of $F_1^{I=0}(t), F_2^{I=0}(t)$

$$F_i^{I=0}(t) = f \left[t; (f_{\omega NN}^{(i)}/f_\omega^e), (f_{\phi NN}^{(i)}/f_\phi^e) \right] \quad (i = 1, 2) \quad (23)$$

where $f_{\omega NN}^{(i)}, f_{\phi NN}^{(i)}$ are coupling constants of ω and ϕ to nucleons and f_ω^e, f_ϕ^e are virtual photon $\leftrightarrow V = \omega, \phi$ coupling constants given by leptonic decay widths $\Gamma(V \rightarrow e^+e^-)$, then the unknown free parameters $(f_{\omega NN}^{(i)}/f_\omega^s), (f_{\phi NN}^{(i)}/f_\phi^s)$ of a strange nucleon FF's model

$$F_i^s(t) = \bar{f} \left[t; (f_{\omega NN}^{(i)}/f_\omega^s), (f_{\phi NN}^{(i)}/f_\phi^s) \right] \quad (i = 1, 2) \quad (24)$$

of the same analytic structure are calculated by the relations (22).

Now, why we use 8-resonance U&A model of nucleon EM structure ?

That follows directly from the derived relations of coupling constant (strange and EM ratios) where always we are determining couples of $\omega - \phi$ strange coupling constants simultaneously. Only 8- 12- etc. resonance U&A models of nucleon EM structure fulfill such restrictions, but in no case 10-resonance one.

All known FF properties are contained consistently in the following specific U&A models

$$\begin{aligned} F_1^{I=0}[V(t)] &= \left(\frac{1 - V^2}{1 - V_N^2} \right)^4 \left\{ \frac{1}{2} L(V_{\omega''}) L(V_{\omega'}) + \right. \\ &[L(V_{\omega''}) L(V_\omega) \frac{(C_{\omega''} - C_\omega)}{(C_{\omega''} - C_{\omega'})} - L(V_{\omega'}) L(V_\omega) \frac{(C_{\omega'} - C_\omega)}{(C_{\omega''} - C_{\omega'})} - \\ &L(V_{\omega''}) L(V_{\omega'})] (f_{\omega NN}^{(1)}/f_\omega^e) + \\ &[L(V_{\omega''}) L(V_\phi) \frac{(C_{\omega''} - C_\phi)}{(C_{\omega''} - C_{\omega'})} - L(V_{\omega'}) L(V_\phi) \frac{(C_{\omega'} - C_\phi)}{(C_{\omega''} - C_{\omega'})} - \\ &L(V_{\omega''}) L(V_{\omega'})] (f_{\phi NN}^{(1)}/f_\phi^e) \left. \right\} \end{aligned} \quad (25)$$

$$\begin{aligned}
F_2^{I=0}[V(t)] &= \left(\frac{1-V^2}{1-V_N^2}\right)^6 \{L(V_{\omega''})L(V_{\omega'})L(V_{\omega}) \\
&[1 - \frac{C_{\omega}}{(C_{\omega''}-C_{\omega'})} \left(\frac{(C_{\omega''}-C_{\omega})}{C_{\omega'}} - \frac{(C_{\omega'}-C_{\omega})}{C_{\omega''}}\right)] \\
&(f_{\omega NN}^{(2)}/f_{\omega}^e) + L(V_{\omega''})L(V_{\omega'})L(V_{\phi}) \\
&[1 - \frac{C_{\phi}}{(C_{\omega''}-C_{\omega'})} \left(\frac{(C_{\omega''}-C_{\phi})}{C_{\omega'}} - \frac{(C_{\omega'}-C_{\phi})}{C_{\omega''}}\right)] \\
&(f_{\phi NN}^{(2)}/f_{\phi}^e)\}
\end{aligned} \tag{26}$$

and

$$\begin{aligned}
F_1^s[V(t)] &= \left(\frac{1-V^2}{1-V_N^2}\right)^4 \\
&\{[L(V_{\omega''})L(V_{\omega}) \frac{(C_{\omega''}-C_{\omega})}{(C_{\omega''}-C_{\omega'})} - L(V_{\omega'})L(V_{\omega}) \frac{(C_{\omega'}-C_{\omega})}{(C_{\omega''}-C_{\omega'})} - \\
&L(V_{\omega''})L(V_{\omega'})](f_{\omega NN}^{(1)}/f_{\omega}^s) + \\
&[L(V_{\omega''})L(V_{\phi}) \frac{(C_{\omega''}-C_{\phi})}{(C_{\omega''}-C_{\omega'})} - L(V_{\omega'})L(V_{\phi}) \frac{(C_{\omega'}-C_{\phi})}{(C_{\omega''}-C_{\omega'})} - \\
&L(V_{\omega''})L(V_{\omega'})](f_{\phi NN}^{(1)}/f_{\phi}^s)\}
\end{aligned} \tag{27}$$

$$\begin{aligned}
F_2^s[V(t)] &= \left(\frac{1-V^2}{1-V_N^2}\right)^6 \{L(V_{\omega''})L(V_{\omega'})L(V_{\omega}) \\
&[1 - \frac{C_{\omega}}{(C_{\omega''}-C_{\omega'})} \left(\frac{(C_{\omega''}-C_{\omega})}{C_{\omega'}} - \frac{(C_{\omega'}-C_{\omega})}{C_{\omega''}}\right)] \\
&(f_{\omega NN}^{(2)}/f_{\omega}^s) + L(V_{\omega''})L(V_{\omega'})L(V_{\phi}) \\
&[1 - \frac{C_{\phi}}{(C_{\omega''}-C_{\omega'})} \left(\frac{(C_{\omega''}-C_{\phi})}{C_{\omega'}} - \frac{(C_{\omega'}-C_{\phi})}{C_{\omega''}}\right)] \\
&(f_{\phi NN}^{(2)}/f_{\phi}^s)\}
\end{aligned} \tag{28}$$

defined each on a four-sheeted Riemann surface with complex conjugate pairs of resonance poles placed only on the unphysical sheets, where

$$\begin{aligned}
L(V_r) &= \frac{(V_N - V_r)(V_N - V_r^*)(V_N - 1/V_r)(V_N - 1/V_r^*)}{(V - V_r)(V - V_r^*)(V - 1/V_r)(V - 1/V_r^*)}, \\
&(r = \omega, \phi, \omega', \omega'') \\
C_r &= \frac{(V_N - V_r)(V_N - V_r^*)(V_N - 1/V_r)(V_N - 1/V_r^*)}{-(V_r - 1/V_r)(V_r^* - 1/V_r^*)}, \\
&(r = \omega, \phi, \omega', \omega'')
\end{aligned}$$

$$V(t) = i \frac{\sqrt{\left[\frac{t_{N\bar{N}} - t_0^{I=0}}{t_0^{I=0}}\right]^{1/2} + \left[\frac{t - t_0^{I=0}}{t_0^{I=0}}\right]^{1/2}} - \sqrt{\left[\frac{t_{N\bar{N}} - t_0^{I=0}}{t_0^{I=0}}\right]^{1/2} - \left[\frac{t - t_0^{I=0}}{t_0^{I=0}}\right]^{1/2}}}{\sqrt{\left[\frac{t_{N\bar{N}} - t_0^{I=0}}{t_0^{I=0}}\right]^{1/2} + \left[\frac{t - t_0^{I=0}}{t_0^{I=0}}\right]^{1/2}} + \sqrt{\left[\frac{t_{N\bar{N}} - t_0^{I=0}}{t_0^{I=0}}\right]^{1/2} - \left[\frac{t - t_0^{I=0}}{t_0^{I=0}}\right]^{1/2}}} \quad (29)$$

$$V_N = V(t)|_{t=0}; V_r = V(t)|_{t=(m_r - i\Gamma_r/2)^2}; (r = \omega, \phi, \omega', \omega''), \quad (30)$$

and $t_{N\bar{N}} = 4m_N^2$ is a square-root branch point corresponding to $N\bar{N}$ threshold.

The expressions for $F_1^{I=0}(t), F_2^{I=0}(t)$ together with similar expressions for $F_1^{I=1}(t), F_2^{I=1}(t)$ are used:

- first to describe Rosenbluth G_{Ep} data in $t < 0$ region together with all other existing nucleon EM FF data with the result $\chi^2/(ndf) = 1.76$
- then JLab proton polarization data on $\mu_p G_{Ep}(t)/G_{Mp}(t)$ in $t < 0$ region together with all other existing nucleon EM FF data with the result $\chi^2/(ndf) = 1.34$.

The results for $G_{Ep}(t)$ $t < 0$ are presented in Fig.8

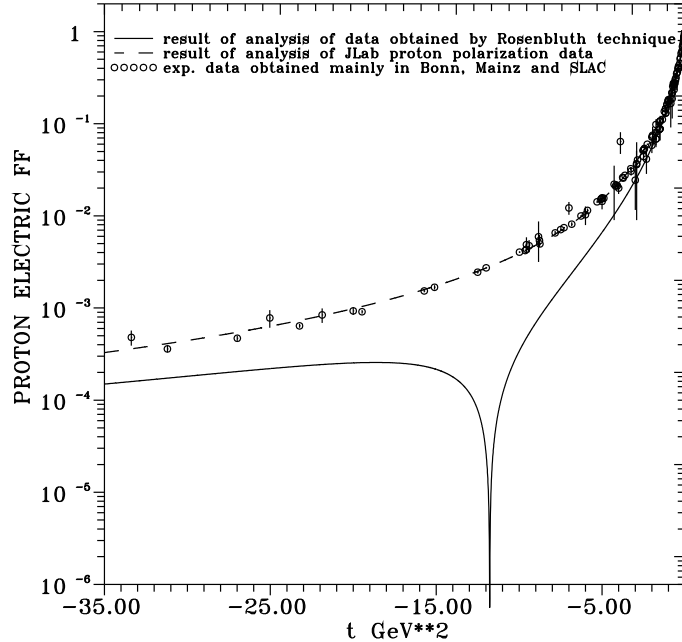


FIG. 8: Results of the analysis of SLAC and JLab data by 8-resonance U&A model

They are similar to the results of the analysis with 10-resonance model, only the zero is shifted from $t = -13\text{GeV}^2$ to $t = -12\text{GeV}^2$.

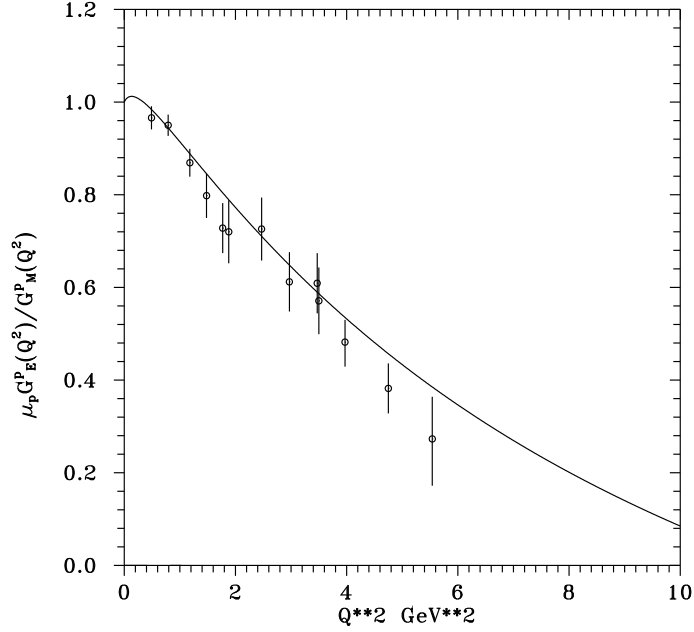


FIG. 9: Description of the JLab proton polarization data by 8-resonance U&A model

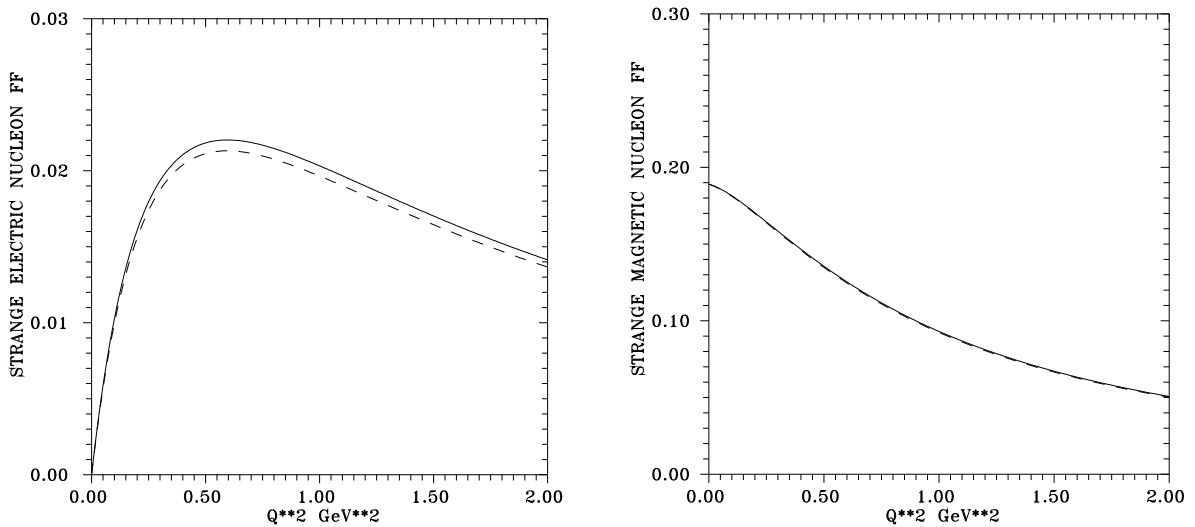


FIG. 10: Theoretical prediction of strange electric and magnetic form factors.

Also a perfect description of the JLab proton polarization data is achieved (see Fig.9).

Now, calculating $(f_{\omega NN}^{(i)}/f_{\omega}^s)$, $(f_{\phi NN}^{(i)}/f_{\phi}^s)$ according to the prescribed procedure and substituting them into the U&A model of strange nucleon FFs, one obtains predictions for behaviors of $G_{EN}^s(Q^2)$ and $G_{MN}^s(Q^2)$ as presented in Fig.10.

As one can see from Fig.10b, a reasonable value of the strangeness nucleon magnetic moment is predicted $\mu_s = +0.19[\mu_N]$.

The behavior of strange nucleon FFs doesn't feel too much the difference in contradicting

behaviors of $G_{Ep}(t)$ in space-like region.

A reasonable description of the recent data on the combination $G_E^s(Q^2) + \eta(Q^2)G_M^s(Q^2)$ for $0.12\text{GeV}^2 < Q^2 < 1.0\text{GeV}^2$ is achieved (see Fig.11) [12]

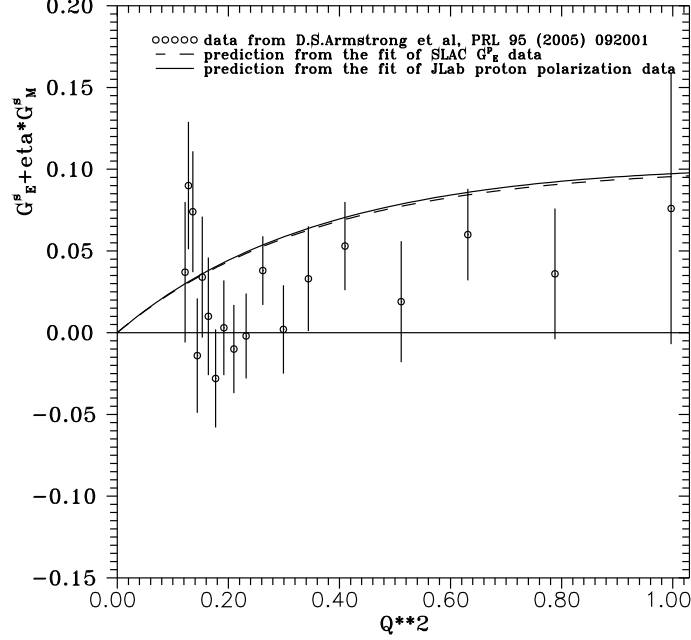


FIG. 11: Prediction for the behavior of the combination of strange nucleon form factors $G_E^s(Q^2) + \eta(Q^2)G_M^s(Q^2)$ by 8-resonance U&A model

VIII. DEUTERON EM STRUCTURE FUNCTIONS DATA AS A JUDGE BETWEEN CONTRADICTIONING $G_E^p(Q^2)$ DATA

The cross-section of elastic electron scattering on deuteron is

$$\frac{d\sigma^{lab}(e^-D \rightarrow e^-D)}{d\Omega} = \frac{\alpha^2 \cos^2(\theta/2)}{4E^2 \sin^4(\theta/2)} \frac{1}{1 + (\frac{2E}{m_D}) \sin^2(\theta/2)} \left[A(t) + B(t) \tan^2(\theta/2) \right] \quad (31)$$

Similarly to the nucleons one can draw out from previous formula the data on $A(Q^2)$ and $B(Q^2)$ as presented in Fig. 12.

The dependence of $A(Q^2)$ and $B(Q^2)$ on deuteron EM FF's is given by the relations

$$\begin{aligned} A(Q^2) &= G_C^2(Q^2) + \frac{8}{9}\eta^2 G_Q^2(Q^2) + \frac{2}{3}\eta G_M^2(Q^2) \\ B(Q^2) &= \frac{4}{3}\eta(1 + \eta)G_M^2(Q^2) \\ \eta &= Q^2/(4m_D^2) \end{aligned}$$

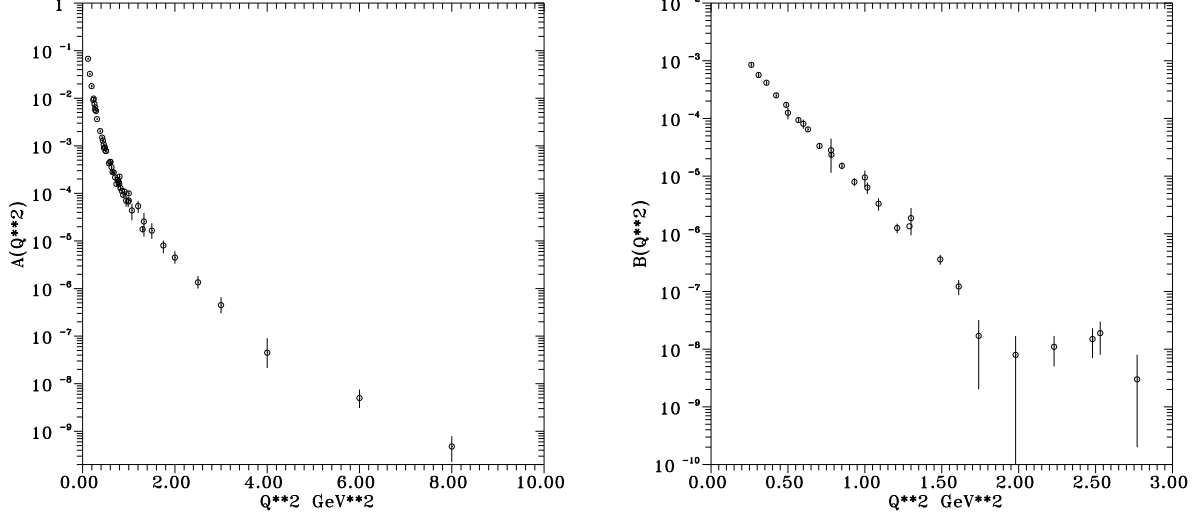


FIG. 12: Experimental data on deuteron EM structure functions.

In the non-relativistic limit deuteron EM FFs can be expressed through the iso-scalar parts ($s \sim I = 0$) of the nucleon electric and magnetic FFs $G_E^s = G_E^p + G_E^n$ and $G_M^s = G_M^p + G_M^n$

$$\begin{aligned}
 G_C &= G_E^s D_C; \\
 G_Q &= G_E^s D_Q; \\
 G_M &= \frac{m_D}{2m_p} (G_M^s D_M + G_E^s D_E)
 \end{aligned}$$

with

$$\begin{aligned}
 D_C(Q^2) &= \int_0^\infty dr [u^2(r) + w(r)] j_0(qr/2) \\
 D_Q(Q^2) &= \frac{3}{\sqrt{2}\eta} \int_0^\infty dr w(r) [u(r) - w(r)/\sqrt{8}] j_2(qr/2) \\
 D_M(Q^2) &= \int_0^\infty dr ([2u^2(r) - w^2(r)] j_0(qr/2) + \\
 &\quad + [\sqrt{2}u(r)w(r) + w^2(r)] j_2(qr/2)) \\
 D_E(Q^2) &= \frac{3}{2} \int_0^\infty dr w^2(r) [j_0(qr/2) + j_2(qr/2)]
 \end{aligned}$$

and $u(r), w(r)$ are the reduced S- and D-state wave-functions.

The set of FFs with the new behavior of $G_E^p(Q^2)$ from the JLab polarization experiments gives a better $\chi^2 = 1404$ in a description of $A(Q^2)$ and $B(Q^2)$ than the set of FFs obtained by Rosenbluth technique $\chi^2 = 2640$.

IX. CONCLUSIONS

- We have presented a manifestation of two contradicting behaviours of $G_E^p(Q^2)$ in various physical phenomena.
- Some of them indicate that the new behavior from the JLab proton polarization experiment with the zero around $t = -12\text{GeV}^2$ seems to be correct.
- However, the source of inconsistency is still left to be confused.

-
- [1] S. Dubnička, A. Z. Dubníčková, P. Weisenpacher, J. Phys. **G29**, 405 (2003).
 - [2] M. K. Jones et al., Phys. Rev. Lett. **84**, 1398 (2000).
 - [3] O. Gayou et al., Phys. Rev. **C64**, 038292 (2001).
 - [4] S.Dubnicka and A.Z.Dubnickova, Fizika B13 (2004) 287.
 - [5] C.Adamuscin, S.Dubnicka, A.Z.Dubnickova, P.Weisenpacher, Prog. Part. Nucl. Physics 55 (2005) 228.
 - [6] P.A.M.Guichon, M.Vanderhaeghen, Phys. Rev. Lett. 91 (2003) 142303-1.
 - [7] P.G.Blunder, W.Melnitchouk, J.A.Tjon, Phys. Rev. Lett. 91 (2003) 142304-1.
 - [8] Y.-C.Chen et al, Phys. Rev. Lett. 93 (2004) 122301-1.
 - [9] M.P.Rekalo, E.Tomasi-Gustafsson, Eur. Phys. J. A22 (2004) 331.
 - [10] S.Dubnicka, E.Kuraev, M.Secansky, A.Vinnikov, hep-ph/0507242.
 - [11] E. Bartoš, S. Dubnička, E. A. Kuraev, Phys. Rev. D **70** (2004) 117901.
 - [12] D.S.Armstrong et al, Phys. Rev. Lett. 95 (2005) 092001.